Front. Earth Sci. 2019, 13(4): 778–790
https://doi.org/10.1007/s11707-019-0797-1

RESEARCH ARTICLE

Factors controlling northward and north-eastward moving tropical cyclones near the coast of East Asia

Qiao LIU[1,2,3], Weican ZHOU[1,2,3], Melinda PENG[4], Tim LI (✉)[5,1,2,3]

1 Collaborative Innovation Center on Forecast and Evaluation of Meteorological Disasters, Nanjing University of Information Science and Technology, Nanjing 210044, China

2 Key Laboratory of Meteorological Disaster Ministry of Education, Nanjing University of Information Science and Technology, Nanjing 210044, China

3 Joint International Research Laboratory of Climate and Environmental Change, Nanjing University of Information Science and Technology, Nanjing 210044, China

4 University of Colorado at Colorado Spring, Colorado Spring, CO 80918, USA

5 International Pacific Research Center and Department of Atmospheric Sciences, School of Ocean and Earth Science and Technology, University of Hawaii at Manoa, Honolulu, HI 96822, USA

Abstract The impacts of multi-time-scale flows on northward and north-eastward moving tropical cyclones (TCs) near the east coast of China in August and September are investigated using reanalysis data from 1982 to 2012. TCs of interest are under the influence of the subtropical high-pressure system in the western North Pacific (WNP). In August when the subtropical high-pressure system is strong and close to the coast line, most TCs in the region move northward, while more TCs move north-eastward in September when the subtropical high-pressure system retreats to the east.

To investigate the influence from different time-scales, the environmental flow is divided into four components, the synoptic flow, the intraseasonal flow, the interannual flow and the climatological background field. Analysis of steering flows between 25°N and 30°N indicates that the meridional steering vectors from all time-scales point to the north, dominated by the intraseasonal component. The deciding factor on whether a TC moves to the north or north-east between 25°N and 30°N is the zonal steering vector. For the northward moving group, the sum of the zonal steering from all time-scales is very small. On the other hand, the north-east moving group has a net eastward zonal component mainly contributed by the climatological mean flow.

Several individual cases that stood out from the majority of the group are analyzed. For those cases, the intraseasonal flow plays an important role in affecting the movement of the TCs mainly through the wave train, in which a cyclonic circulation is located to the north-west (north) and an anticyclonic circulation to the south-east (east) of TCs. The analysis of the steering vectors indicates the importance of all components with different time-scales to the movement of TCs.

Keywords northward moving TC, north-eastward moving TC, steering flow

1 Introduction

About one-third of global tropical cyclones (TCs) form in the western North Pacific (WNP) each year (Chan, 2005; Maue, 2011). TCs can bring serious threats to human lives and damage properties along the coast. As a TC approaches the eastern Asian coast, a key operational forecast challenging is whether it will keep a mainly north-west movement and landfall in China, or a northward movement hitting Korea, or recurve north-eastward to affect Japan. The purpose of this study is to identify essential factors that control the TC track at this critical junction.

Formed over the low-latitude tropical warm ocean, TCs usually take a mainly westward or north-westward motion in the early stage due to the beta effect and trade easterly winds (Holland, 1983; Chan and Williams, 1987; Fiorino and Elsberry, 1989; Williams and Chan, 1994). Previous studies indicate that many factors can affect the movement of a TC. Anthes (1982) indicated that the most important factor controlling the TC motion is the steering flow from

Received April 9, 2019; accepted October 7, 2019

E-mail: timli@hawaii.edu

the environment. The advection of a TC by its environment is closely related to the vertically averaged wind field between 850 hPa and 300 hPa (Holland, 1984). Wang et al. (1998) identified the averaged horizontal wind within 5°–7° latitude radius from the cyclone center as optimal to represent the environmental steering flow. In addition, the interaction between the convergent flow of a TC and the planetary vorticity gradient causes a westward deviation from the pure steering flow (Holland, 1983). Li and Zhu (1991) suggested that the asymmetric TC structure also contributes to its movement. Lander and Holland (1993) provided a common model of the binary interaction between TCs. Zhang et al. (2013) categorized three groups of parameters that affect the TC recurvature, including the large-scale circulation, circulations surrounding TCs and variables near the core of TCs. By using the tree construction algorithm, 18 rules have been identified to governing the TC recurvature.

It has been shown that the intraseasonal oscillation (ISO) is a prominent mode in the atmosphere in the WNP (Li and Wang, 2005; Li, 2010 and 2014; Hsu and Li, 2011; Cao et al., 2014) and often has a significant impact on TC tracks (Kim et al., 2008; Tao et al., 2012; Li and Zhou, 2013; Yoshida et al., 2014; Yang et al., 2015; Bi et al., 2015). Kim et al. (2008) found that a dense area of tracks may migrate westward when the ISO convection is located near the tropical WNP. Yang et al. (2015) revealed that the majority of TCs in the South China Sea move westward following the overall background TC steering flow, while some move eastward under the influence of the ISO. Bi et al. (2015) demonstrated that the interaction between Typhoon Megi (2010) and an intraseasonal-scale monsoon gyre plays the critical role in the sharp northward turning of Megi.

El Ninõ-Southern Oscillation (ENSO) is one of the most important interannual time-scale oceanic and atmospheric variabilities and it can affect TC motions (Camargo et al., 2007; Takahashi and Shirooka, 2014; Yonekura and Hall, 2014). Wang and Chan (2002) pointed out that TCs may form more in the eastern sub-region of the WNP and are more likely to recurve northward to higher latitudes under the El Ninõ influence. Wang et al. (2013) investigated the variability of TC steering flows associated with various ENSO events. During the early season of warm eastern Pacific years, the TC steering flow patterns favor the recurving track and suppress the straight westward and north-westward tracks. During the TC peak season, warm eastern Pacific episodes are associated with the steering flows unfavorable for TCs to move north-westward or westward, whereas central Pacific warming favors the north-westward track and suppresses the straight westward track.

Observations show that some TCs in the WNP moved northward from 25°N to 30°N within a narrowed longitudinal band along the east coast of China. Some of these storms continued moving northward and affected Korean Peninsula and North-east China, while others recurved to the east and affected Japan (Fig. 1). Due to the critical impacts these storms may have along the coast of eastern Asia, we will investigate mechanisms behind these TC movements from multi-scale environmental flow perspective and shade lights on what determines these different tracks.

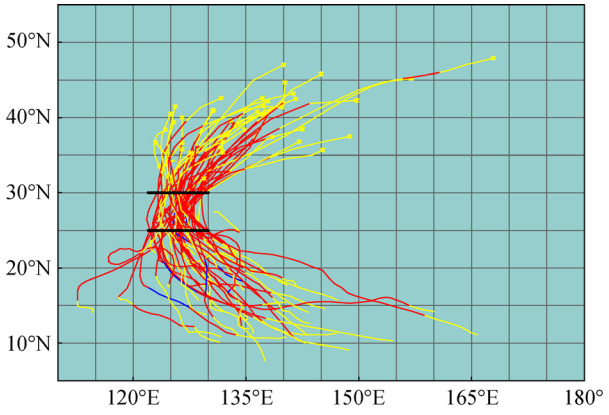

Fig. 1 TC tracks during the active TC season (from June to November) of 1982–2012 near the east coast of China (blue lines represent the super typhoon category, red lines represent the typhoon category and yellow lines represent the tropical storm category).

The remaining part of this paper is organized as follows. The data and methodology, and the classification of north-eastward and northward TC tracks are described in Section 2. Section 3 demonstrates differences of the environmental flows between northward and north-eastward moving TCs. In Section 4, the characteristics of distinctive TC tracks and climatological background flows in August and September are investigated. Section 5 examines the contributions of steering flows with different time-scales to cases of special interest in August and September. Finally, a summary is presented in Section 6.

2 Data and methodology

2.1 Data

The primary data sets used in this study are the ERA-Interim reanalysis (Dee et al., 2011), produced by European Centre for Medium-Range Weather Forecast (ECMWF) with 1.5° × 1.5° grid resolution at 6-h intervals for the period of 1982–2012. The major meteorological fields are multi-level horizontal wind fields from 850 hPa to 300 hPa and they are used to compute the steering flow and vorticity fields. The TC information comes from the best track data set of the Joint Typhoon Warning Center (JTWC), including storm positions and intensities at a 6-h interval. The TC genesis time is defined as when the maximum tangential wind reaches to 17.2 m/s (about 33

knots). The analysis is confined to the active TC season of WNP between June to November (JJASON).

2.2 Methodology

The analysis focuses on TCs that traveled near the east coast of China between 25°N and 30°N without hitting China. TCs whose track intersected with both the line segment of 25°N, 122–130°E and 30°N, 122–130°E (black lines in Fig. 1) are chosen in our study. Based on these criteria, 47 TCs during the active TC season in 1982–2012 are selected (Fig. 1). These TCs formed in the region between 7°N and 19°N and later moved northward or recurved to high latitudes beyond 30°N.

Based on the direction of TC movement and the affected area after TCs have passed 30°N along the China coast, the selected TCs are divided into two groups. The first group contains 27 TCs, identified as the northward moving TCs, which moved northward after crossing the 30°N line shown in Fig. 1. Northward moving TCs mainly affected South Korea, North Korea and part of the north-east China (Fig. 2(a)). The second group contains 18 north-eastward moving TCs that mainly affected the southern area of Japan after passing 30°N (Fig. 2(b)). There were two TCs that weakened quickly north of 30°N and have been removed in the classification. There were also several TCs classified as northward moving TCs that landed in South or North Korea first and then also made landfall in Japan but we still put them in the northward moving group.

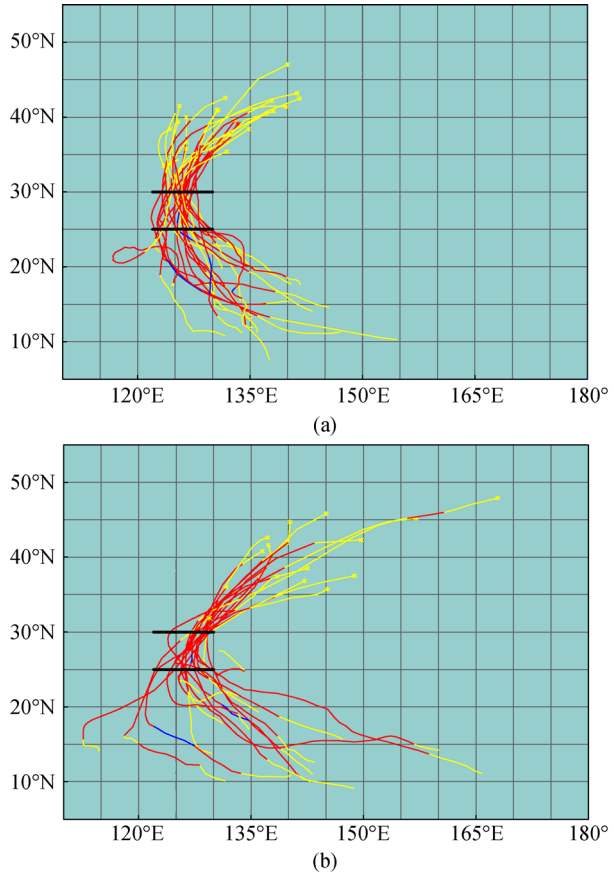

Fig. 2 Same as Fig. 1 but (a) for northward-moving and (b) north-eastward-moving TCs

We compute the TC steering flow as the horizontally averaged wind field within a radius of 500 km and vertically averaged between 850 hPa and 300 hPa (Holland, 1984; Bi et al., 2015; Liu et al., 2018) with the centers of tropical cyclones as determined by the JTWC. We also compute the steering flow using 700–400 hPa as the vertical range, and a radius of 700 km and obtain similar results. To analyze the influence of the background flow on TC tracks, we apply a 10-day low-pass filter (Duchon, 1979) to remove the TC circulation and other synoptic flows. To examine the structure and evolution of the multi-time-scale steering flows, a 10–90-day band-pass Lanczos filter and a 90-day low-pass Lanczos filter (Duchon, 1979) are applied to the original data respectively. By separating flows with different time-scales, one may examine the relative impacts of them on the TC movement. The environmental flow is separated into three components, a climatological monthly mean background field which has been 90-day low-pass filtered, an interannual component obtained by subtracting the climatological background field from the 90-day low-pass filtered field, and an intraseasonal (10–90-day band-pass filtered) component. The total field also includes the synoptic flow (10-day high-pass filtered) with periods less than 10 days. The TC component has been filtered out in the synoptic flow to obtain the synoptic steering flow using the TC-removal method by Kurihara et al. (1995).

3 Environmental flows for northward and north-eastward moving TCs

The vertically averaged horizontal winds from 850 hPa to 300 hPa with the 10-day low-pass filtered are composited for TCs that have passed 30°N from the south (Fig. 1) for the northward (Fig. 2(a)) and north-eastward (Fig. 2(b)) moving TCs. An anticyclonic circulation representing the subtropical high dominates the entire WNP for both the northward and the north-eastward moving groups (Fig. 3). The subtropical high tends to be stronger in summer than in winter especially in the North Pacific (Miyasaka and Nakamura, 2005) and September is situated in the transition phase. The 5880 m geopotential height, a typical representation of the position of the subtropical high-pressure system in the western Pacific, shows a distinction between the northward moving group and the north-westward moving group north of 25°N. For the northward TC group, the anticyclonic circulation extended more to the north and west and thus enhanced the southerly wind in the area of interest (blue box, Fig. 3(a)), contributing to the northward movement in this group. On the other hand, the more south-eastward-shifted position of the anticyclonic

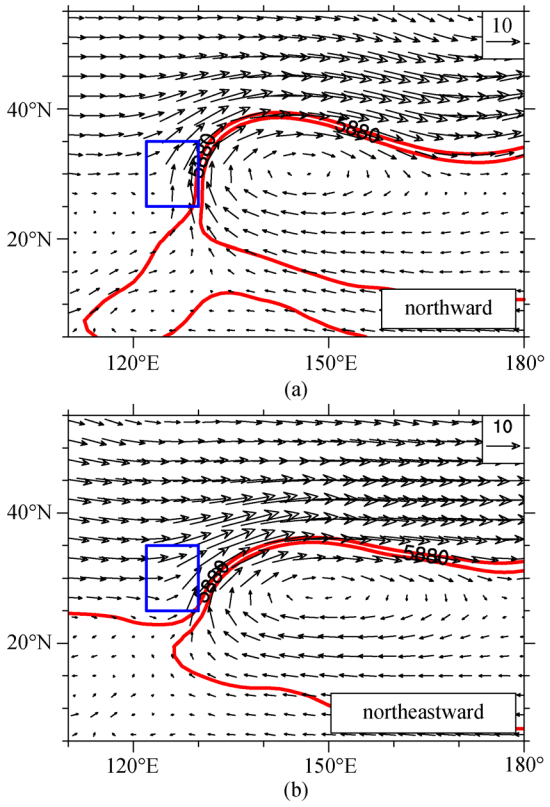

Fig. 3 Composite vertically averaged (850–300 hPa) horizontal wind fields (10-day low-pass filtered, vector; unit: m/s) and the 500 hPa geopotential height (red curve; unit: m) patterns for (a) northward and (b) north-eastward moving TCs after TCs passed 30°N. Blue boxes represent the region of (25°N–35°N, 122°E–130°E).

system for the north-eastward moving TCs (Fig. 3(b)) post a wider range of westerlies in the mid-latitude and in the area of interest. The strengthened westerly flow near the east coast of China is conducive to guide a TC to move more eastward.

The domain averaged horizontal wind is computed over the region of (25°N–35°N, 122°E–130°E), within the blue box marked in Fig. 3. Table 1 lists the magnitudes of zonal and meridional flows from the background field for the northward and north-eastward moving TCs. The southerly steering speed in the environment is larger than the zonal component for the northward moving TCs, consistent with their northward movement. Meanwhile the averaged eastward flow of the north-eastward moving TCs is greater than its southerly. The averaged eastward speed of the environment for the north-eastward moving TCs is 5.47 m/s, while it is about 1.6 m/s for the northward moving TCs. The averaged northward speed of the environment for the northward moving TCs is twice as large as that of the north-eastward moving TCs, contributing to the overall northward movement.

In summary, the large-scale environmental flows show significant difference between the northward and north-eastward moving TC groups, especially in the region of interest, and thus are responsible for the TC movement. The change of the environmental flow near the east coast of China is closely related to the position of the anticyclonic circulation associated with the subtropical high-pressure system over the WNP. A north-westward extension of the anticyclone would lead to a strengthened northward steering flow on the west side of the anticyclonic circulation and guide a TC to move northward. Meanwhile, a south-eastward retreat of the anticyclone would lead to a strengthened eastward steering flow, favoring a TC to move in the same direction.

4 Influence of multi-scale steering flows on TC movements

For TC cases passed 30°N coming from the equator side during 1982–2012, we further examine their moving directions in individual months from June to November (Fig. 4). While it is not surprising that most of the TCs occurred in August and September, the monthly distribution displays a clear distinction between the northward moving group and the north-eastward moving group, with the number of cases peaks in August for the former group and peaks in September for the latter. The trend of peaking for the northward moving group is ahead of the north-eastward group. Overall, the number of northward TCs is greater than the number of north-eastward TCs with the largest contribution coming from August.

To reveal the influence of the climatological background field on TC tracks, the vertically averaged horizontal wind from 850 hPa to 300 hPa, with 90-day low-pass filtered, is monthly averaged for 1982 to 2012. Figure 5 shows the monthly mean flows in August and September, illustrating that the difference of the anticyclonic circulation between them. Since August is dominated by northward moving TCs while September is dominated by north-eastward moving TCs (Fig. 4), the climatological background flows

Table 1 Averaged zonal and meridional flows from the background fields for northward and north-eastward moving TCs over the region of (25°N–35°N,122°E–130°E) and averaged zonal and meridional flows from the climatological background fields in August and September over the region of (25°N–35°N,122°E–130°E)

	Northward moving TC	North-eastward moving TC	August	September
Zonal component (U; m/s)	1.60	5.47	1.38	4.64
Meridional component (V; m/s)	5.04	2.52	1.85	0.85

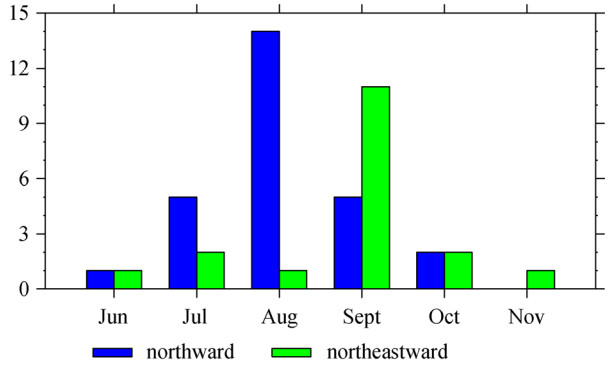

Fig. 4 Numbers of northward and north-eastward moving TCs in different months (Statistical numbers were counted based on the time when TCs passed 30°N). Blue bars represent the northward moving TCs and green bars represent the north-eastward moving TCs.

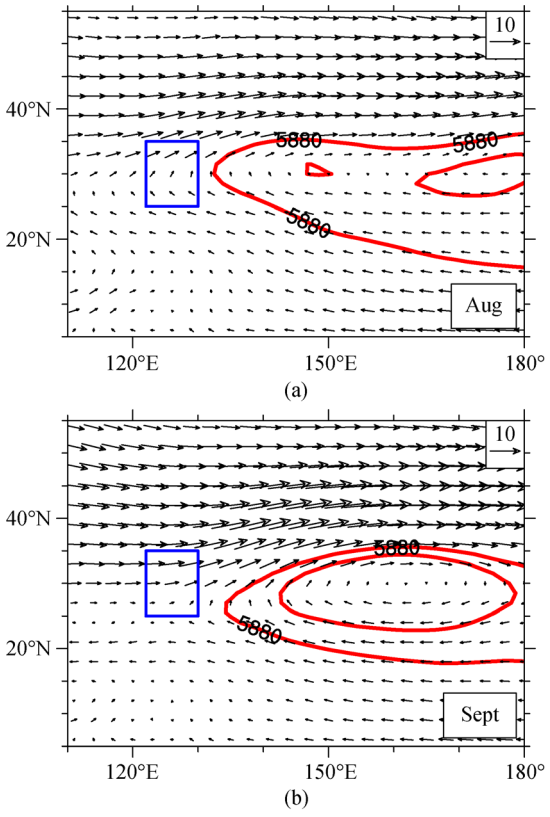

Fig. 5 Composite of the vertically averaged (850–300 hPa) climatological horizontal background flows (vector; unit: m/s) and the 500 hPa geopotential height (red curve; unit: m) patterns in (a) August and (b) September. Blue boxes represent the region of (25°N–35°N, 122°E–130°E).

of August and September bear some similarities to the composites of the two TC groups (Fig. 3), especially within the area of interest (blue box). This reflects how different large-scale surrounding flows at different time control the TC movements. The enhanced southerly wind in August is associated with the westward extension of the anticyclone, indicating that TCs are more likely to move northward near the east coast of China (Fig. 5(a)). The westward extension of the subtropical high also causes more northward TCs in July (Figure not shown). The eastward withdrawing of the subtropical high-pressure system in September brings stronger westerlies at mid-latitudes and drives TCs north-eastward (Fig. 5(b)).

To quantify the difference of the climatological mean flows between August and September near the east coast of China, the domain average wind speed is computed over the region of (25°N–35°N, 122°E–130°E). Table 1 lists the amplitudes of the zonal and meridional steering flows within the box marked in Fig. 5 for August and September. In August, the mean flow has an averaged meridional speed of 1.85 m/s, while the average speed of the eastward component is 1.38 m/s. Meanwhile, the averaged zonal speed of 4.64 m/s for September is three times that of August. The westerly flow is also larger than the southerly flow in the same month, contributing to a north-eastward movement of TCs. Note that there are also many TC cases in September that moved northward, even though they are in an environment with a relatively larger zonal wind speed climatologically. These cases will be examined in Section 5.

The influences of different time-scale flows on the movement of the two types of TCs between 25°N and 30°N are examined. Chan and Gray (1982) and other studies (George and Gray, 1976 and 1977; Lander and Holland, 1993; Chan, 1985; Carr and Elsberry, 1995) indicate that the steering flow is the key indicator of the direction of TC movement. The steering vectors also vary with different definitions (Chan, 1985). Composite steering vectors with different time-scales, including the synoptic scale and the actual moving vectors are computed and displayed in Fig. 6.

First noticeable characteristics of the meridional steering components is that nearly all of them with different time-scales are positive, pointing to the north. This is not surprising as we are looking at TCs moving in general in the northward direction, but are trying to distinguish between northward and north-eastward TCs. For the meridional steering, the largest contribution comes from the intraseasonal flow.

Since we are investigating contributions of different time-scales leading to the northward verse the north-eastward TC movement between 25°N and 30°N and all the meridional components are pointing to the north, the deciding factor falls on the zonal component of the steering (Fig. 6(b)). In the N_Aug group, all the zonal steering vectors are small, making the total steering vector pointing to the north and the group has the largest number of northward moving TCs (Fig. 4). The N_Sept group has the climatological and the synoptic steering pointing to the east, but cancelled by the interannual and intraseasonal

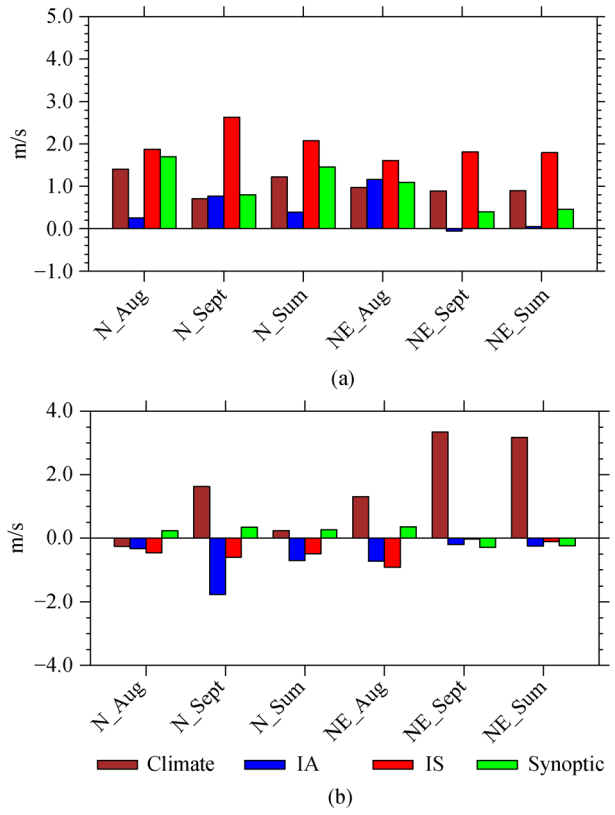

Fig. 6 Composites of the (a) meridional and (b) zonal climatological background, interannual, intraseasonal and synoptic steering flows (unit: m/s) when TCs were located between 25°N and 30°N. Brown bars represent the climatological background flows, blue bars represent the interannual flows, red bars represent the intraseasonal flows and green bars represent the synoptic flows. "N_Aug" and "N_Sept" represent the northward-moving TCs in August and September. "NE_Aug" and "NE_Sept" represent the north-eastward-moving TCs in August and September. "N_Sum" and "NE_Sum" represent the total northward and north-eastward moving TCs.

westward steering so that the total zonal steer speed is very small and TCs moved to the north. The NE_Aug group contains only one storm and it will be further examined in Section 5. For the NE_Sept group, the climatological steering dominates with an eastward component and TCs in this group moved north-eastward.

In summary, the meridional steering vectors from all time-scales point to the north and are dominated mainly by the intraseasonal component. The deciding factor on whether a TC moves to the north or north-east is the zonal steering vector. For the northward moving group, the sum of the zonal steering from all time-scales is very small. On the other hand, the north-eastward moving group has a net eastward zonal component mainly contributed by the climatological mean flow. In general, the climatological background flow and the synoptic flow in this region point to the east (except for the N_Aug group with a very small climatological steering to the west and the NE_Sept group with westward synoptic steering), while the zonal steering of intraseasonal and interannual component points to the west. The outcome is determined by the combined influence of all time-scales in the zonal direction.

5 Impacts of multi-scale steering flows on individual TC cases

While TCs in August are dominated by the northward movement and TCs in September are dominated by the north-eastward movement, there are one north-eastward moving TC in August and five northward moving TCs in September that warrant more detailed investigations. We examine how the steering flows associated with different time-scales affect the movement of these individual TCs as they moved north of 30°N.

5.1 North-eastward moving TCs in August

On 1200 UTC 05 August 1996, Kirk was identified as a tropical storm by the JTWC. The center of Kirk was located at 27.5°N, 130.7°E. This is different from most of the TCs which were originated from the south. Kirk moved south-eastward and was upgraded to the typhoon category (winds greater than 64 knots) on 0000 UTC 08 August. Kirk curved to the west and moved toward the east coast of China from 0000 UTC 08 to 1800 UTC 12 August. Kirk then moved north-eastward and landed in Japan (Fig. 7) among TCs in August when most of TCs moved northward in a generally more northward climatological mean flow (Fig. 5(a)). To analyze the influence of multi-time-scale flows on Kirk, we examine the structure and evolution of the intraseasonal and the interannual flows and their relations with the movement of Kirk. The climatological component during the lifetime of Kirk is similar to the one shown in Fig. 5(a).

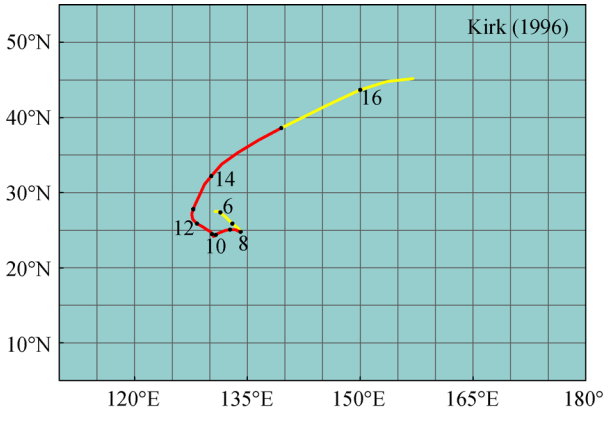

Fig. 7 Track of the north-eastward moving TC Kirk (1996) in August. Red lines represent the typhoon category and yellow lines represent the tropical storm category. Black dot denotes the generation location of TC center. The numbers indicate the dates in August 1996.

The evolution of the intraseasonal flow from 30°N to 35°N for Kirk (1996) is shown in Fig. 8. A slowly moving wave train (WT), with a cyclonic circulation located to the north-west of Kirk and an anticyclonic circulation situated to the south-east of Kirk, resulting a north-eastward steering (Figs. 8(a)–8(c)). Kirk moved north-eastward under the influence of the intraseasonal WT and landed in Japan at 0000 UTC 14 August. The influence of the WT pattern to the TC motion can be seen in the composite constructed with respect to the storm center when Kirk was located between 25°N and 30°N from 1200 UTC 13 August to 1200 UTC 14 August (Fig. 8(d)).

Figure 9(a) displays the averaged interannual flow of Kirk when it was traveling between 25°N and 30°N. A cyclonic circulation was located to the east of Japan and a weak anticyclonic circulation near the east coast of China. This pattern is quite different from the composite for the intraseasonal flow shown in Fig. 8. This northerly flow associated with the interannual flow is against the north-eastward steering associated with the climatological flow. To obtain a complete picture of the steering, all different time-scale components are plotted, including the synoptic-scale flow (Fig. 9(b)). Except for the small southward steering from the interannual flow and a north-westward steering of the synoptic flow, the intraseasonal and the climatological steering components point to the north-east, causing a north-eastward movement of Kirk. Beyond 35°N, Kirk was affected by the large westerly north-west of the subtropical high-pressure system. The main difference between Fig. 9(b) constructed for Kirk (1996) and the steering with different time-scales shown in Fig. 6 for the NE_Aug group is that the results in Fig. 6 were computed for Kirk (the only TC in August that moved north-eastward) within 25°N and 30°N and Figs. 9(b) were for 30°N–35°N.

Our analysis here indicates that the intraseasonal flow, the interannual flow, and the synoptic flow can contribute differently and guide Kirk to move eastward and limit the northward movement of it, resulting in a north-eastward track. Therefore, all components of the steering flow are important to TC movement. Note that the northward and eastward moving speeds of Kirk can be, to a large extent,

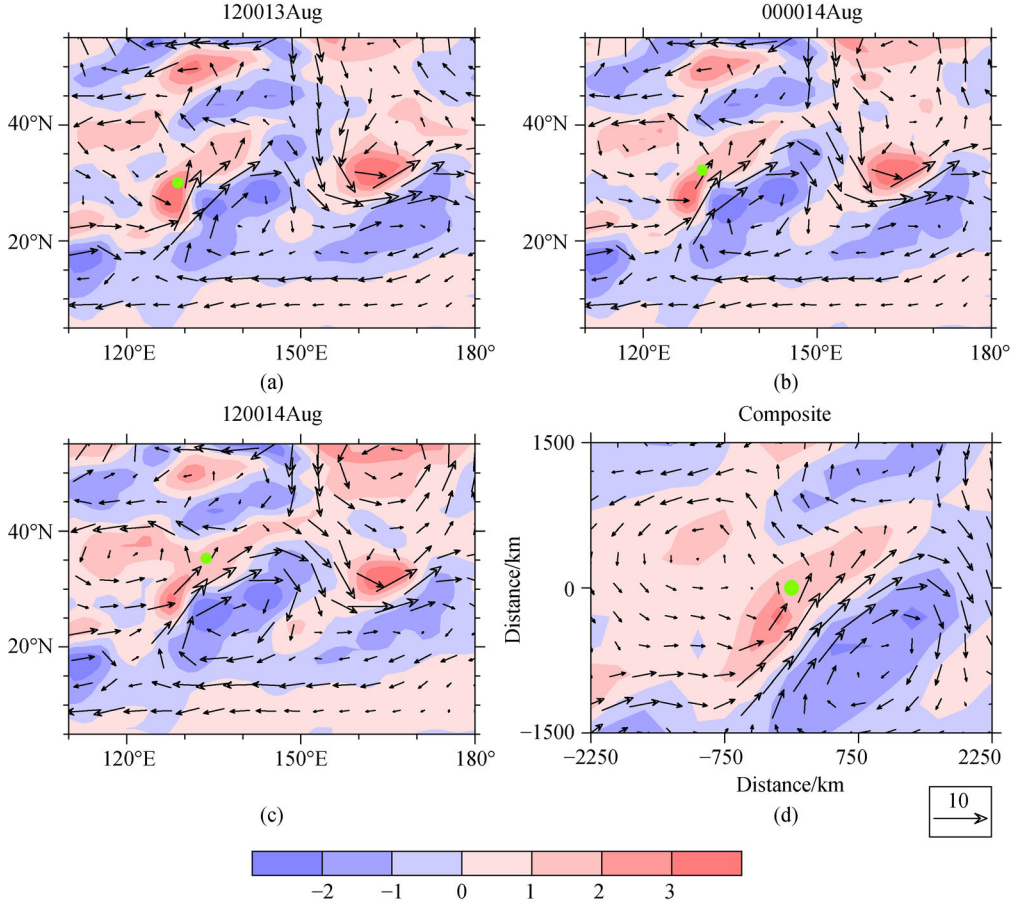

Fig. 8 Evolution of vertically averaged (850 hPa to 300 hPa) intraseasonal wind (vector, unit: m/s) and vorticity (shaded, unit: 10^{-5} /s) fields for Typhoon Kirk (1996) (a–c) and the composite field (d) when Kirk was located between 25°N and 30°N from 1200 UTC 13 August to 1200 UTC 14 August based on the TC center. Green dot denotes the location of Kirk's center.

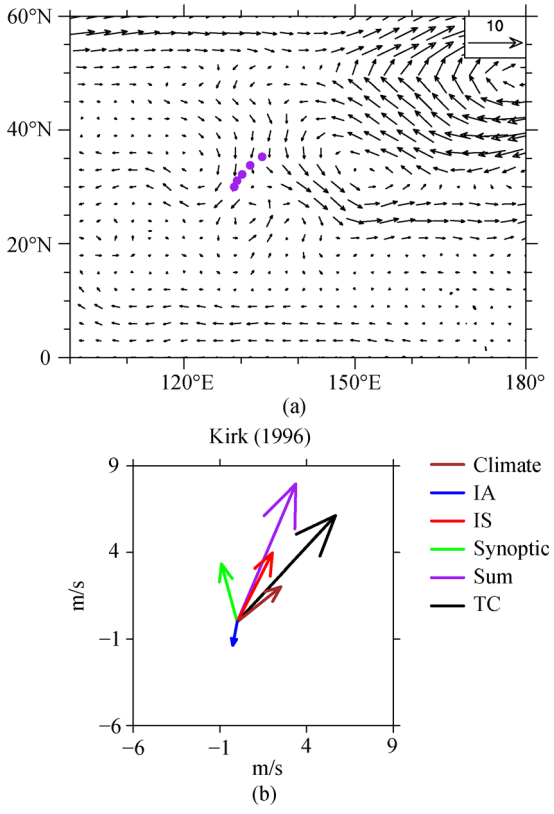

Fig. 9 Averaged interannual wind (a, vertically averaged from 850 hPa to 300 hPa, unit: m/s) field when Kirk was located between 25°N and 30°N from 1200 UTC 13 August to 1200 UTC 14 August and steering vectors with different time-scales and the actual moving vector (b, unit: m/s) for Krik from the best track data. (Purple dot denotes the location of Kirk's center. (0, 0) denotes the center of Kirk. "Climate," "IA," "IS," "Synoptic," "Sum" and "TC" represent the steering vector of the climatological mean flow in August (brown), the interannual flow (blue), the intraseasonal flow (red), the synoptic flow (green), the sum of all fields (purple) and the actual motion of Krik (black), respectively.

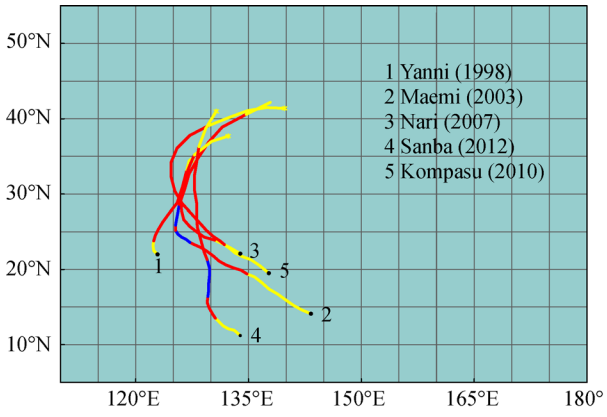

Fig. 10 Tracks of five northward moving TCs in September (blue lines represent the super typhoon category, red lines represent the typhoon category and yellow lines represent the tropical storm category).

explained by the sum of the synoptic, intraseasonal, interannual and climatological background flow components. The north-eastward steering flow is largely contributed by the climatological background flow and the intraseasonal flow.

5.2 Northward moving TCs in September

There are five northward moving TCs occurred in September (Fig. 10) during the period when the north-eastward moving TCs dominate. These storms moved against the climatological north-eastward flows near the east coast of China within our cases shown in Fig. 4. First, the structure and evolution of the intraseasonal flows for the five northward moving TCs are analyzed. We found that a zonal oriented WT, with a cyclonic circulation to the west and an anticyclonic circulation to the east, existed in all the five northward moving TC cases, contributing to the northward movement of TCs. As the effects of intraseasonal flows on these northward moving TCs are similar, TC Nari (2007) is selected to illustrate the detailed analysis.

Figure 11 shows the intraseasonal flow and vorticity fields of Nari (2007). There was negative vorticity appeared near Japan, while positive vorticity existed near Philippines and east of China, consisting a WT throughout the period of 1200 UTC 15 to 0000 UTC 17 September. The orientation of the WT is from south-east to north-west and Nari was advected by the south-easterly from the intraseasonal flow, moving along with the southerly band and landing in South of Korean Peninsula at 1200 UTC 16 September. And then Nari moved northward continually, under the influence of northward flow associated with the WT. The intraseasonal south-easterly associated with the south-east-north-west oriented WT is obvious in the composite fields centered on Nari (Fig. 11(f)). It steers Nari to move against the climatological south-easterly flow of September, resulting a northward track.

Figure 12 illustrates the composited interannual flow between 1200 UTC 15 to 0000 UTC 17 September after Nari moved to 30°N. An interannual anticyclonic circulation was located near south of Japan and South of Korea and an interannual cyclonic circulation near Taiwan, China, contributing to a long easterly band around 30°N. Strong westward flow near the east coast of China favored the westward movement of a TC, against the eastward steering of the climatological background flow of September. Eventually, Nari landed in south of Korean Peninsula.

The structure of the intraseasonal flow of Sanba (2012) shows a similar WT pattern as for Nari (2007). The intraseasonal WT, in which a cyclonic circulation was located to the west and an anticyclonic circulation to the east, contributed to the northward movement of Sanba. The pattern can be seen in the composite intraseasonal steering

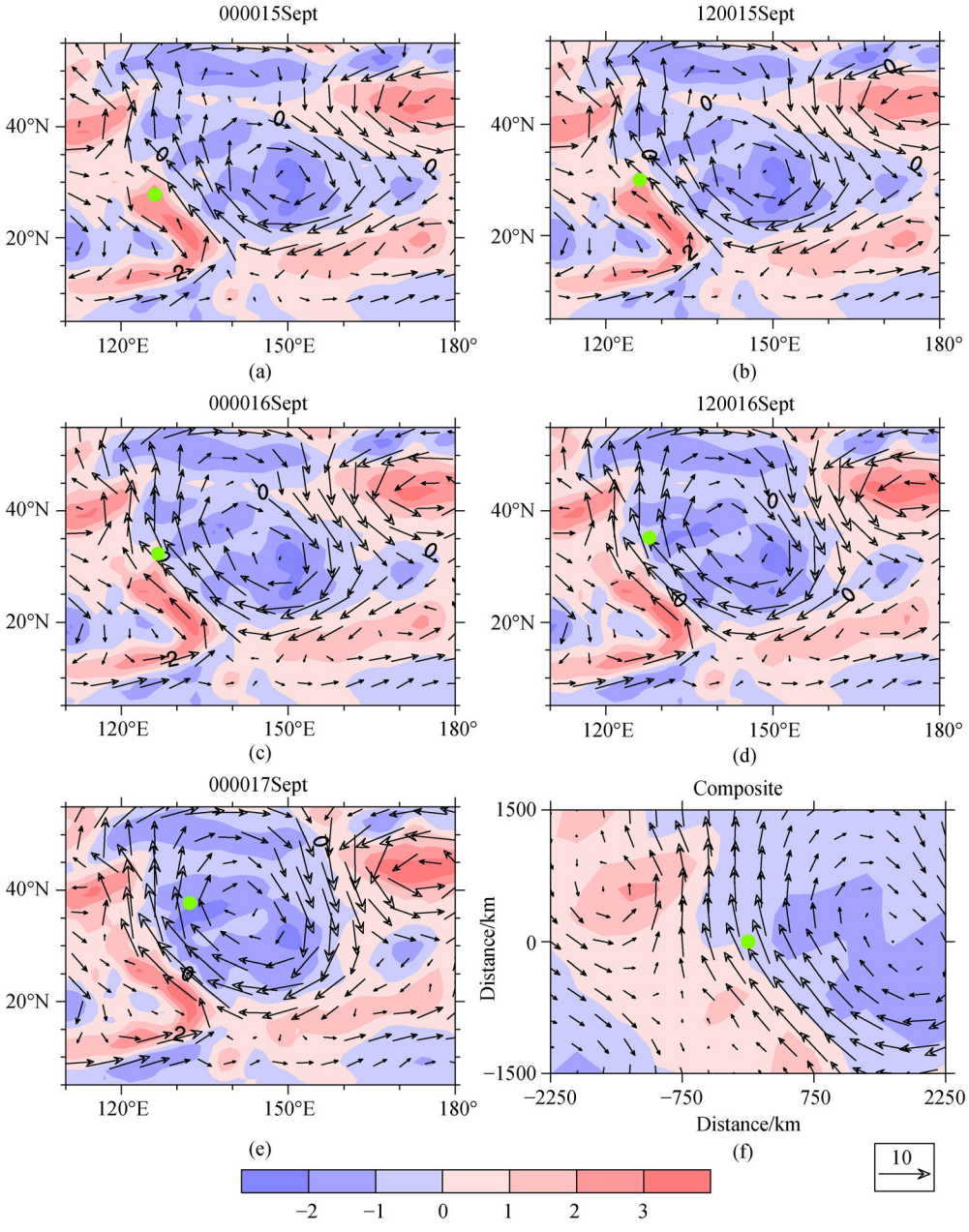

Fig. 11 Same as Fig. 8, but for Nari (2007). fig.8 (f) displays the composite field from 1200 UTC 15 to 0000 UTC 17 September after Nari passed 30°N.

flow based on the center of Sanba (Fig. 13(a)). Sanba was also under the influence of the interannual anticyclone located north of Japan. Figure 13(b) is the averaged interannual flow from 1200 UTC 16 to 1800 UTC 17 September after Sanba passed 30°N, illustrating a strong anticyclone to the north of Japan and a weak cyclonic circulation to the south-west of South Korea. Sanba was located to the south of South Korea, moving northward under the influence of the north-westward flow associated with the interannual circulations. The southerly and easterly flows near the east coast of China enhance the northward component and weaken the eastward component of the climatological flow (Fig. 5(b)), leading to the northward movement of Sanba in September.

The composite SST (sea surface temperature) anomaly of these five northward moving TCs displays a La Niña pattern (Fig. 14). According to the Gill response, the negative heating anomaly in the central Pacific can affect subtropical anticyclone in the WNP, causing an anomaly of it. The enhanced south-easterly near the east coast of Asia associated with the anomalous anticyclone helps TCs to move northward, consistent with the Sanba case shown in

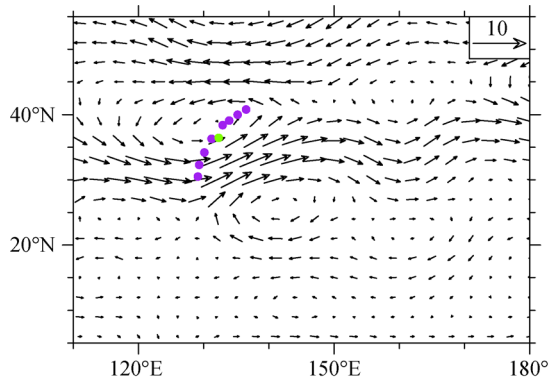

Fig. 12 Averaged interannual wind field (vertically averaged from 850 hPa to 300 hPa; unit: m/s) after the TC passed 30°N from 1200 UTC 15 to 0000 UTC 17 September. Purple dot denotes the location of Nari's (2007) center, and the green dot denotes the averaged location of Nari's (2007) center.

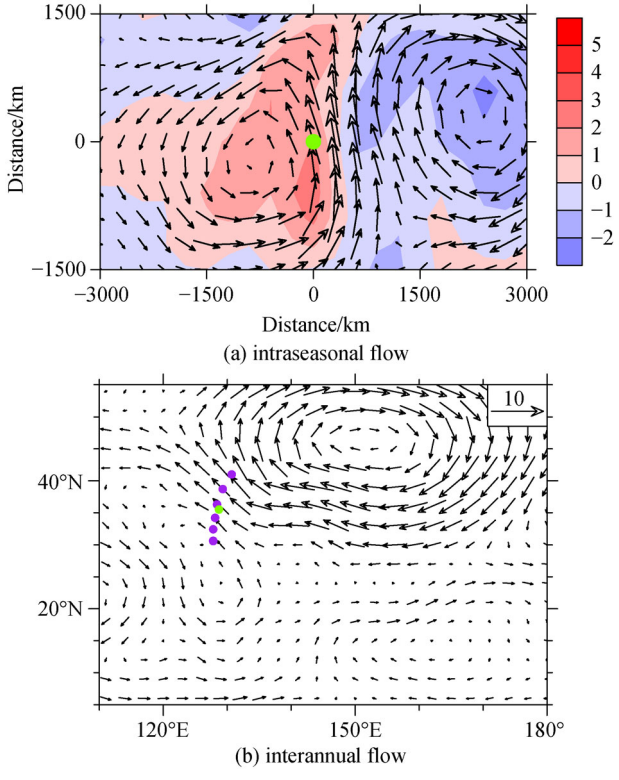

Fig. 13 Composite of the vertically averaged (850 hPa to 300 hPa) (a) intraseasonal wind (vector, unit: m/s) and vorticity (shaded, unit: 10^{-5} /s) fields for Sanba (2012) based on the TC center and (b) interannual wind (unit: m/s) field based on grids after the TC passed 30°N from 1200 UTC 16 to 1800 UTC 17 September. Purple dot denotes the location of Sanba's (2012) center, and the green dot denotes the averaged location of Sanba's (2012) center.

Fig. 13. The positive SST anomaly near the east coast of China can induce a barotropic anomaly anticyclone, causing the interannual easterly near 40N. The easterly south of the anomalous anticyclone also reduces the climatological westerly, leading to the positive SST anomaly.

To investigate the relative importance of different time-scale steering flows contributing to the unusual northward TC tracks in September, the steering vectors for the five TC cases are computed (Fig. 15). We confine our composites for computing the steering vectors for TCs located south of 35°N so that they do not include the time that TCs recurved to the north-east in their late stage. Compared with actual moving speeds of TCs, the sum of the synoptic, intraseasonal, interannual and climatological background flows can represent the TC movement well. The sums of the total steering from the analysis fields are always to the right of the best track vectors for the five cases. Observational studies showed that in most cases, TCs in the Northern Hemisphere move to the left of the steering current (George and Gray, 1976; Chan and Gray, 1982). The westward deviation from the steering flow is caused by the interaction between TCs and the Earth's vorticity field. Since our illustration is a composite instead of instantaneous, some deviation is expected. The strong climatological eastward steering flow favors the eastward movement of TCs, while the zonal components of the intraseasonal and interannual steering flows for the five TC cases are mostly to the west. The synoptic, intraseasonal, interannual and climatological flows all play different roles in contributing to northward TC tracks in September (Fig. 15). Among the five cases, Sanba has the most diversified distribution of the steering vectors from different time-scales. A separated study is devoted to it.

6 Conclusions and discussion

In this study, we examine the influences of multi-time-scale flows on TCs off east coast of China that moved northward from 25°N to 30°N and were located between 122°E and 130°E. The TCs we investigated from 1982 to 2012 are divided into two groups, the northward and the north-eastward moving groups. The northward moving TCs moved northward after crossing the 30°N line and affected South Korea, North Korea and the north-east of China, while north-eastward moving TCs moved north-eastward beyond 30°N and mainly affected Japan.

The surrounding environmental flow affects the northward and north-eastward moving TCs primarily through the changes of the location of the anticyclonic circulation over the WNP associated with the subtropical high-pressure system. A north-westward extension (south-eastward withdraw) of the anticyclone would lead to the strengthened northward (eastward) flow west of the anticyclonic circulation, guiding TCs to move northward (north-eastward). Most northward moving TCs appeared in August, while most north-eastward moving TCs occurred in September. The differences of the TC movement between

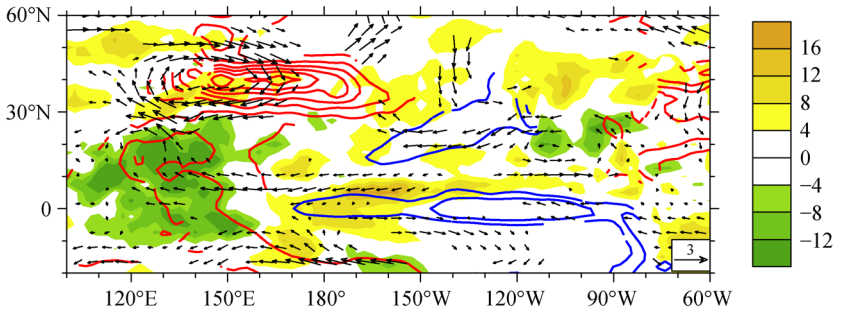

Fig. 14 Composite of the vertically averaged (850 hPa to 300 hPa) interannual wind vectors (unit: m/s) for the five northward moving TCs, sea surface temperature anomalies (contour; unit: °C; interval: 0.5 °C) and outgoing longwave radiation anomalies (shading; unit: W/m^2) in September. The red lines represent the positive sea surface temperature anomalies and the blue lines represent the negative sea surface temperature anomalies. The region exceeding the 90% confidence level is shown.

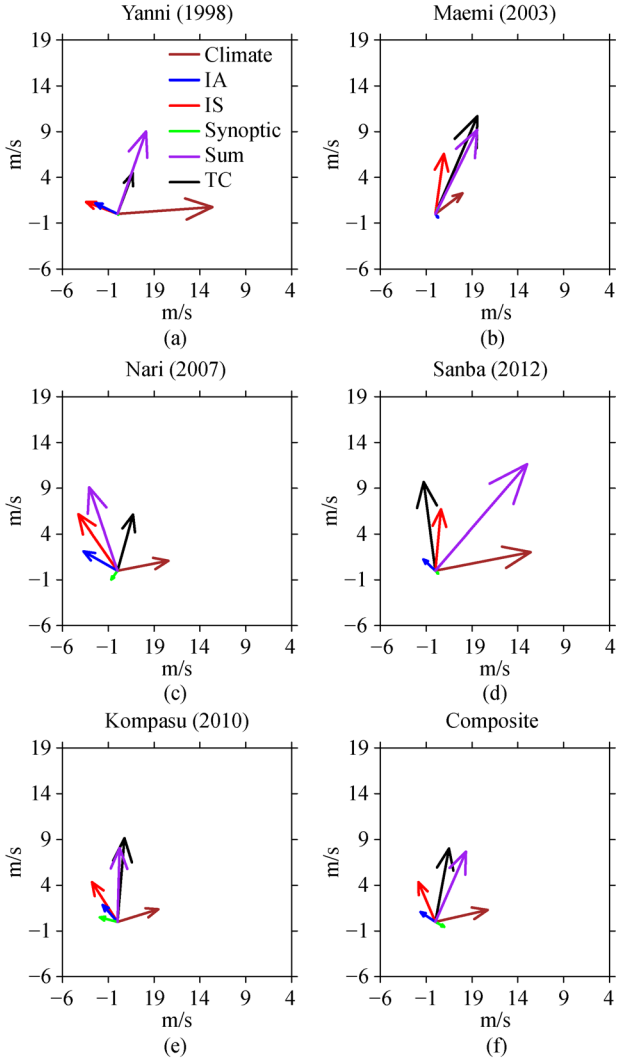

Fig. 15 Steering vectors (unit: m/s) with different time-scales and the actual moving vectors for five northward moving TCs (a–e) in September. (f) Displays the composite result of (a–e). ("Climate," "IA," "IS," "Synoptic," "Sum" and "TC" represent the steering vector of the climatological mean flow in September (brown), the interannual flow (blue), the intraseasonal flow (red), the synoptic flow (green), the sum of all steering vectors (purple) and the actual motion of TCs (black) respectively).

August and September are affected by the change of the climatological background flow in these two months. The westward (eastward) shift of the anticyclone is associated with the stronger (weaker) northward and weaker (stronger) eastward flows, contributing to more northward (north-eastward) TC tracks in August (September).

To investigate the influence of different time-scale flows on the movement of the two types of TC movement between 25°N and 30°N, the environmental flow is separated into four components, the synoptic component, the intraseasonal component, the interannual component and the climatological background field. The meridional steering from four components all points to the north and is largely contributed by the intraseasonal component. The zonal steering of northward moving TCs is nearly zero, while the north-eastward moving TCs are steered by the eastward zonal flow mainly contributed by the climatological background flow. Thus, the difference of the moving direction between northward and north-eastward moving TCs is attributed to the direction of the zonal components of the steering flows.

There are one north-eastward moving TC occurred in August among the mostly northward storms and five northward moving TCs in September among the mostly north-eastward moving storms. By examining the surrounding flows and the steering vectors with different time-scales of each case, we find that the intraseasonal, the interannual, and the synoptic flows play different roles in contributing to individual TC tracks, enhancing the north-eastward steering of north-eastward moving TCs in August and enhancing the northward steering and reducing the eastward steering of northward moving TCs in September. The intraseasonal steering appears to play a critical role in these unusual TC cases.

Overall, the sum of all steering vectors from different time-scales conforms well to the TC moving vector. From a modeling perspective, all time-scales are important in determining the movement of a tropical cyclone with their relative importance changing with time and locations of the storm. An in-depth investigation for Typhoon Sanba (2012), mentioned briefly here, follows the present study.

Acknowledgements This work was jointly supported by National Key R&D Program of China (Grant Nos. 2018YFC1505800 and 2015CB453200), NOAA (No. NA18OAR4310298), National Science Foundation (No. AGS-1643297), National Natural Science Foundation of China (Nos. 41630423 and 41875069), and NRL (Grant No. N00173-16-1-G906) and China Scholarship Council (Grant No. N201908320496). This is SOEST contribution number 10834, IPRC contribution number 1409 and ESMC number 285.

References

Anthes R A (1982). Tropical cyclones: their evolution, structure and effects. Amer Meteor Soc Meteorological Monographs, 19: 208

Bi M Y, Li T, Peng M, Shen X Y (2015). Interactions between Typhoon Megi (2010) and a low-frequency monsoon gyre. J Atmos Sci, 72(7): 2682–2702

Camargo S J, Robertson A W, Gaffney S J, Smyth P, Ghil M (2007). Cluster analysis of typhoon tracks. Part II: large-scale circulation and ENSO. J Clim, 20(14): 3654–3676

Cao X, Li T, Peng M, Chen W, Chen G H (2014). Effects of monsoon trough intraseasonal oscillation on tropical cyclogenesis in the western North Pacific. J Atmos Sci, 71(12): 4639–4660

Carr L E III, Elsberry R L (1995). Monsoonal interactions leading to sudden tropical cyclone track change. Mon Weather Rev, 123(2): 265–290

Chan J C L (1985). Identification of the steering flow for tropical cyclone motion from objectively analyzed wind fields. Mon Weather Rev, 113(1): 106–116

Chan J C L (2005). Interannual and interdecadal variations of tropical cyclone activity over the western North Pacific. Meteorol Atmos Phys, 89(1–4): 143–152

Chan J C L, Gray W M (1982). Tropical cyclone movement and surrounding flow relationships. Mon Weather Rev, 110(10): 1354–1374

Chan J C L, Williams R T (1987). Analytical and numerical studies of the beta-effect in tropical cyclone motion. Part I: zero mean flow. J Atmos Sci, 44(9): 1257–1265

Dee D P, Uppala S M, Simmons A J, Berrisforda P, Polia P, Kobayashib S, Andraec U, Balmasedaa M A, Balsamoa G, Bauera P, Bechtolda P, Beljaarsa A C M, van de Bergd L, Bidlota J, Bormanna N, Delsola C, Dragania R, Fuentesa M, Geera A J, Haimbergere L, Healya S B, Hersbacha H, Holm E V, Isaksena L, Kallberg P, Kohler M, Matricardia M, McNallya A P, Monge-Sanzf B M, Morcrettea J J, Parkg B K, Peubeya C, de Rosnaya P, Tavolatoe C, Thepaut J N, Vitarta F (2011). The ERA-Interim reanalysis: 391 Configuration and performance of the data assimilation system. Quart. J. Roy. 392 Meteor. Q J Roy Meteor Soc, 137: 553–597

Duchon C E (1979). Lanczos filtering in one and two dimensions. J Appl Meteorol, 18(8): 1016–1022

Fiorino M, Elsberry R L (1989). Some aspects of vortex structure related to tropical cyclone motion. J Atmos Sci, 46(7): 975–990

George J E, Gray W M (1976). Tropical cyclone motion and surrounding parameter relationships. J Appl Meteorol, 15(12): 1252–1264

George J E, Gray W M (1977). Tropical cyclone recurvature and nonrecurvature as related to surrounding wind-height fields. J Appl Meteorol, 16(1): 34–42

Holland G J (1983). Tropical cyclone motion: environmental interaction plus a beta effect. J Atmos Sci, 40(2): 328–342

Holland G J (1984). Tropical cyclone motion: a comparison of theory and observation. J Atmos Sci, 41(1): 68–75

Hsu P C, Li T (2011). Interactions between boreal summer intraseasonal oscillations and synoptic-scale disturbances over the western North Pacific. Part II: apparent heat and moisture sources and eddy momentum transport. J Clim, 24(3): 942–961

Kim J H, Ho C H, Kim H S, Sui C H, Park S K (2008). Systematic variation of summertime tropical cyclone activity in the western North Pacific in relation to the Madden-Julian oscillation. J Clim, 21(6): 1171–1191

Kurihara Y, Bender M A, Tuleya R E, Ross R J (1995). Improvements in

the GFDL hurricane prediction system. Mon Wea Rrev, 123(9): 2791–2801

Lander M, Holland G J (1993). On the interaction of tropical-cyclone-scale vortices. Part I: observations. Quart J Roy Meteor Soc, 119(514): 1347–1361

Li R C Y, Zhou W (2013). Modulation of western North Pacific tropical cyclone activity by the ISO. Part II: tracks and landfalls. J Clim, 26(9): 2919–2930

Li T, Zhu Y (1991). Analysis and modeling of tropical cyclone motion. Part I: asymmetric structure and sudden change of tracks. Sci China, 34(2): 222–233 (Series B)

Li T, Wang B (2005). A review on the western North Pacific monsoon: synoptic-to-interannual variabilities. Terr Atmos Ocean Sci, 16(2): 285–314

Li T (2010). Monsoon climate variabilities. Climate Dynamics: Why Does Climate Vary, 10: 27–51

Li T (2014). Recent advance in understanding the dynamics of the Madden-Julian oscillation. J Meteor Res, 28(1): 1–33

Liu Q, Li T, Zhou W C (2018). Impact of 10–60-day low-frequency steering flows on straight northward-moving typhoon tracks over the western North Pacific. J Meteor Res, 32(3): 394–409

Maue R N (2011). Recent historically low global tropical cyclone activity. Geophys Res Lett, 38(14): 14803

Miyasaka T, Nakamura H (2005). Structure and formation mechanisms of the Northern Hemisphere summertime subtropical highs. J Clim, 18(23): 5046–5065

Takahashi C, Shirooka R (2014). Storm track activity over the North Pacific associated with the Madden-Julian Oscillation under ENSO conditions during boreal winter. J Geophys Res D Atmospheres, 119(18): 10,663–10,683

Tao L, Li S J, Han Y, Wu M (2012). Impact of intraseasonal oscillations of tropical atmosphere on TC track change over the western North Pacific. J Trop Meteorol, 28(5): 698–706

Wang B, Chan J C (2002). How strong ENSO events affect tropical storm activity over the western North Pacific. J Clim, 15(13): 1643–1658

Wang B, Elsberry R L, Wang Y Q, Wu L G (1998). Dynamics in tropical cyclone motion: A review. Chin J Atmos Sci, 22(4): 535–547

Wang C Z, Li C X, Mu M, Duan W S (2013). Seasonal modulations of different impacts of two types of ENSO events on tropical cyclone activity in the western North Pacific. Clim Dyn, 40(11–12): 2887–2902

Williams R T, Chan J C (1994). Numerical studies of the beta effect in tropical cyclone motion. Part II: zonal mean flow effects. J Atmos Sci, 51(8): 1065–1076

Yang L, Du Y, Wang D, Wang C, Wang X (2015). Impact of intraseasonal oscillation on the tropical cyclone track in the South China Sea. Clim Dyn, 44(5–6): 1505–1519

Yonekura E, Hall T M (2014). ENSO effect on East Asian tropical cyclone landfall via changes in tracks and genesis in a statistical model. J Appl Meteorol Climatol, 53(2): 406–420

Yoshida R, Kajikawa Y, Ishikawa H (2014). Impact of boreal summer intraseasonal oscillation on environment of tropical cyclone genesis over the western North Pacific. Sola, 10(0): 15–18

Zhang W, Leung Y, Chan J C L (2013). The analysis of tropical cyclone tracks in the western North Pacific through data mining. Part I: Tropical cyclone recurvature. J Appl Meteorol Climatol, 52(6): 1394–1416